



Citation for published version:

Ding, H, Zang, J, Jin, P, Ning, D & Zhao, X 2021, 'On the performance of an integrated cylinder WEC-type breakwater system', Paper presented at 36th International Workshop on Water Waves and Floating Bodies, 25/04/21 - 28/04/21.

Publication date:
2021

[Link to publication](#)

University of Bath

Alternative formats

If you require this document in an alternative format, please contact:
openaccess@bath.ac.uk

General rights

Copyright and moral rights for the publications made accessible in the public portal are retained by the authors and/or other copyright owners and it is a condition of accessing publications that users recognise and abide by the legal requirements associated with these rights.

Take down policy

If you believe that this document breaches copyright please contact us providing details, and we will remove access to the work immediately and investigate your claim.

On the performance of an integrated cylinder WEC-type breakwater system

Haoyu Ding^{1*}, Jun Zang¹, Peng Jin², Dezhi Ning³, Xuanlie Zhao²

1 Department of Architecture and Civil Engineering, University of Bath, BA2 7AY, U.K.

* E-mail: hd484@bath.ac.uk.

2. College of Shipping Engineering, Harbin Engineering University, Heilongjiang, 150001, China.

3. State Key Laboratory of Coastal and Offshore Engineering, Dalian University of Technology, Dalian, 116024, China

HIGHLIGHTS

This study aims to optimise an integrated cylinder WEC-type breakwater system. Two numerical methods, computational fluid dynamics method and potential flow theory-based method, are used and compared first in this abstract. Then, the parametric investigations are implemented by using potential flow theory-based method.

1 INTRODUCTION

Wave energy converters (WECs) are built to extract wave energy. However, this kind of devices is still expensive for commercial utilisations. To cut down the cost of WECs by sharing the construction-cost with breakwaters, an integrated WEC-type breakwater system (hereafter WEC-B system) is proposed to extract wave energy and attenuate incident waves. This study investigates the performance of wave energy extraction of an WEC-B system, which comprises the heaving oscillating buoys attached at the weather side of a truncated breakwater. Both computational fluid dynamics (CFD) tool, OpenFOAM[®], and the potential flow theory-based solver, HAMS[®], are utilised to optimise the performance of the WEC-B system. Both of these numerical tools are validated by comparing with the experimental data obtained from Zhao et al. (2019).

In our computations, OpenFOAM[®] provides the viscosity corrections for the potential flow solver by using decay tests. With the viscosity corrections, HAMS[®] can be significantly improved to predict the heave responses of the heaving oscillating buoys and to calculate the efficiency of wave energy extraction with different incident waves of this WEC-B system more accurately. In this way, the investigation by using the modified HAMS[®] saves huge amount of computational time compared with using CFD tool, OpenFOAM[®] itself. Thus, HAMS[®] is employed to the parametric study on the WEC-B system for the optimisation of this integrated system. The effect of gap width between the WEC buoy and the breakwater, geometry of the WEC buoy and coaxial cylinder buoys setup on the efficiency of wave energy extraction of the WEC-B system will be investigated and discussed in this workshop.

2 NUMERICAL MODEL

For OpenFOAM[®], the solver, *interFoam*, is employed to simulate fluid-structure interactions. Waves are generated and dissipated by using the relaxation-based wave generation toolbox *waves2Foam* proposed by Jacobsen et al. (2012). The Navier-Stokes equations, which is introduced below, are utilised for *interFOAM* to describe the motion of fluid continuum. These equations are written as a mass conservation equation and momentum equation by Newton's second law, which are showed below respectively:

$$\nabla \cdot \vec{U} = 0 \quad (1)$$

$$\frac{\partial \rho \vec{U}}{\partial t} + \nabla \cdot (\rho \vec{U} \vec{U}) - \nabla \cdot (\mu \nabla \vec{U}) - \rho \vec{g} = -\nabla p - \vec{f}_\sigma \quad (2)$$

where \vec{U} is the flow velocity vector, ρ is the density of fluid, μ refers to the dynamic viscosity, \vec{g} is the acceleration of gravity, p is the pressure of fluid, and the last term \vec{f}_σ denotes the surface tension which has minor effects in civil engineering issues. Thereinto, three components of the velocity vector in three dimensions of Cartesian coordinates and the fluid pressure are unknown variables in governing equations. And OpenFOAM[®] utilises the finite volume method to solve these equations in the Eulerian meshes.

For HAMS[®], the potential flow theory with the assumption that the flow is inviscid, irrotational and incompressible is governed by the velocity potential $\Phi(\mathbf{x}, t)$ which satisfies:

$$\nabla^2 \Phi = 0 \quad (3)$$

For the regular waves, the complex velocity potential $\phi(\mathbf{x})$ can be related to $\Phi(\mathbf{x}, t)$ by:

$$\Phi = \text{Re}(\phi e^{-i\omega t}) \quad (4)$$

where ω is the frequency of the incident waves and t is time. In terms of complex velocity potential, the boundary-value problem can be expressed in the frequency domain:

$$\phi = \phi_0 + \phi_7 + i\omega \sum_{j=1}^6 \zeta_j \phi_j \quad (5)$$

where ϕ_0 is the incident potential, ϕ_7 is the diffraction potential, ζ_j ($j = 1, \dots, 6$) are six rigid body motions and ϕ_j ($j = 1, \dots, 6$) are six radiation potential components. The velocity potential components are subjected to the following boundary conditions at the free surface, on the body surface, at the seabed and in the Sommerfeld condition respectively:

$$\left\{ \begin{array}{l} \frac{\partial \phi}{\partial z} \Big|_{z=0} = v\phi \\ \frac{\partial \phi}{\partial n} \Big|_{S_B} = V_n \\ \frac{\partial \phi}{\partial z} \Big|_{z=-h} = 0 \text{ or } \lim_{z \rightarrow \infty} \left(\frac{\partial \phi}{\partial z} \right) = 0 \\ \lim_{R \rightarrow \infty} \left[\sqrt{vR} \left(\frac{\partial \phi}{\partial R} - i v \phi \right) \right] = 0 \end{array} \right. \quad (6)$$

where $v = \omega^2/g$, g is the acceleration of gravity, V_n refers to the normal velocity at a point on the immersed body boundary S_B , h denotes the water depth and R is the horizontal distance from the body. This boundary-value problem in HAMS[®] is solved by a standard boundary integral equation approach (Liu, 2019; Liu et al., 2016)

In our computations, the heave motion of the heaving oscillating WEC buoy is required to calculate capture width ratio (*CWR*), which is used to evaluate the efficiency of wave energy extraction. The heave motion can be yielded from the following equation:

$$(-\omega^2(M + \mu_0) - i\omega(\lambda + \lambda_{PTO}) + K)\zeta = F_{EX} \quad (7)$$

where M is mass, μ_0 denotes added mass, λ and λ_{PTO} are wave damping and damping of power take off (PTO) system respectively, K is buoyance stiffness, ζ refers to motion of structure and F_{EX} denotes wave excited force. The F_{EX} is obtained from HAMS[®] by solving potential flow theories as the following equation:

$$F_{EX} = \rho i \omega \int_{S_0} (\phi_0 + \phi_7) ds \quad (8)$$

where ρ is the density of fluid and S_0 denotes the area of the bottom of cylinder WEC in this study. While the μ_0 and λ , which are influenced by viscosity, are calculated by the free decay test in OpenFOAM[®]. The μ_0 is calculated from the free decay time period, $T_0 = 2\pi\sqrt{(M + \mu_0)/K}$ and the $\lambda = \frac{2\kappa K}{\omega_0}$, where $\omega_0 = 2\pi/T_0$, $\kappa = \frac{1}{2\pi} \ln \left(\frac{z_i - z_{i-1}}{z_{i-2} - z_{i-3}} \right)$, z_i are the successive peak or trough values of the heave response in the free decay test. In this way, the ζ can be obtained from Eq. (7) with viscosity corrections. As for the optimal damping of PTO system λ_{PTO} , because the generated power by the motion of WEC can be denoted as $P_{capture} = \frac{1}{2} \lambda_{PTO} \omega^2 |\zeta|^2$, The optimal λ_{PTO} can be defined as:

$$\lambda_{PTO} = \sqrt{(K/\omega - \omega(M + \mu_0))^2 + \lambda^2} \quad (9)$$

The *CWR* is calculated as the ratio of the generated power by the motion of WEC to the incident wave power.

3 VALIDATION OF NUMERICAL MODEL

The sketch of the setup of WEC-B system is shown in Figure 1. For the setup of validation cases, the heaving oscillating cylinder WEC buoys with radius of 0.135 m and draft of 0.2 m are installed in front of a fixed truncated breakwater with the draft of 0.25 m and the structure breadth of 0.6 m. The gap width between the cylinder WEC buoys and the breakwater is 0.1 m, the water depth (h) is 1 m and the incident wave height is kept a constant value of 0.12 m.

Figure 2 shows the mesh setup of the 3D numerical wave tank in OpenFOAM[®]. The *oversetMesh* is utilised in this simulation. The *oversetMesh* consists of two sets of mesh: 1) the *overset mesh* which is around the floating structure and

has the same movement with the floating structure; 2) the background mesh which is static mesh. The data information is transferred between two sets of mesh. In term of *oversetMesh* setup, the deformation of mesh in the narrow gap can be avoided, which allows OpenFOAM® to be able to simulate these WEC-B system test cases more accurately.

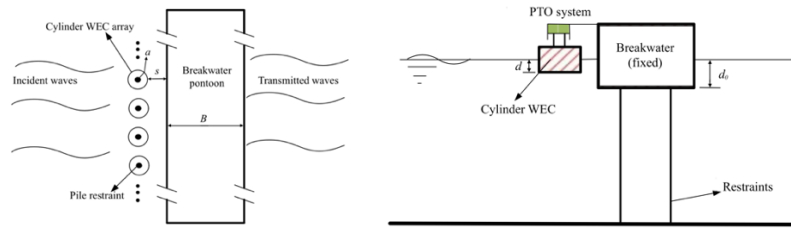


Figure 1. the top view (left) and side view (right) of the integrated cylinder WEC-type breakwater system.

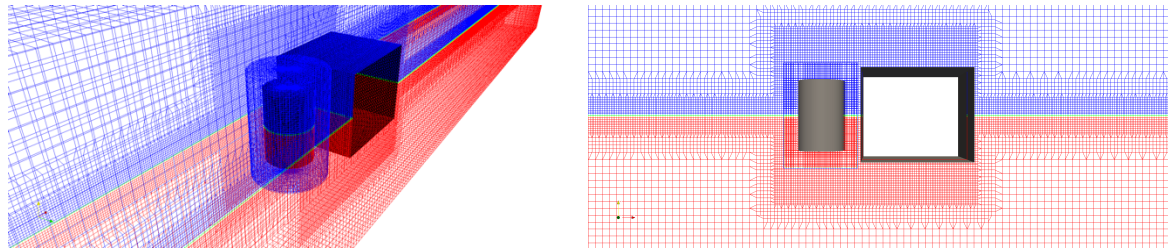


Figure 2. the background mesh and overset mesh setup in OpenFOAM®.

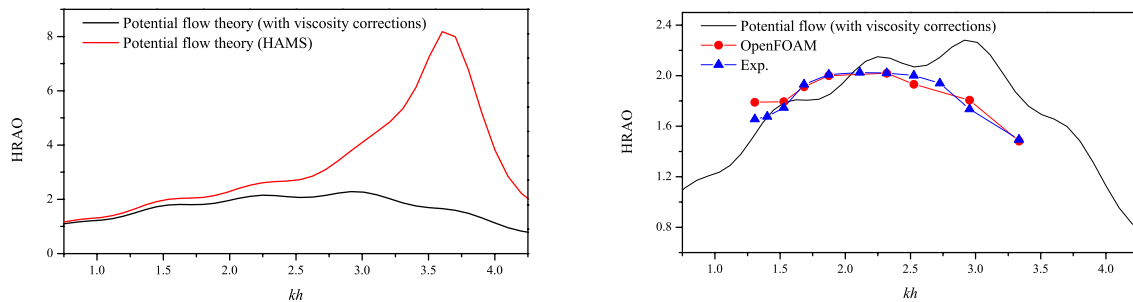


Figure 3. comparison of HRAO as a function of kh (k is wave number, h is water depth).

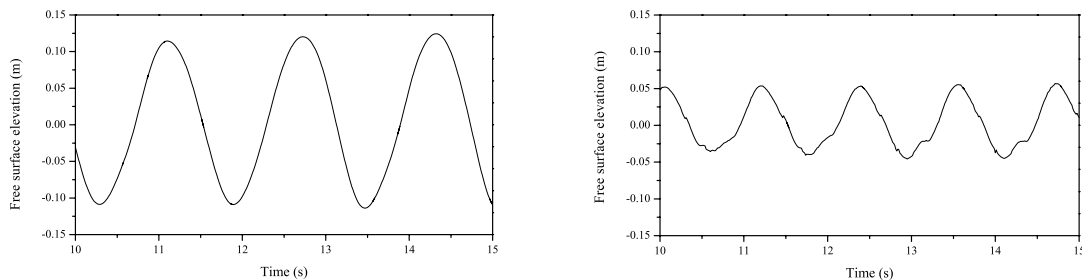


Figure 4. the free surface elevation in the gap between cylinder WEC and breakwater in time history when incident wave period is 1.60 s (left) and 1.17 s (right).

The left-hand side diagram in Figure 3 shows that the heave response amplitude operator calculated by the potential flow theory-based method ($HRAO = \text{heave response of structure} / \text{incident wave amplitude}$) decreases sharply after including the viscosity corrections, especially around the nature frequency of the cylinder WEC buoy. The right-hand side diagram in Figure 3 validates the results calculated by the potential flow solver with viscosity corrections and by the CFD method with the experimental data (Zhao et al., 2019). In the lower wave frequency region ($kh < 2.5$), both HAMS® and OpenFOAM® results have a good agreement with experimental data. In the higher wave frequency region ($kh > 2.5$), the OpenFOAM® results still predicts the HRAO accurately compared with experimental results, however, the results of HAMS® are higher than the results of OpenFOAM® and experiments. The overestimation of HRAO by HAMS® may be influenced by the complex wave conditions in the narrow gap between the cylinder WEC and the breakwater. Figure 4 shows two time histories of free surface elevation in the narrow gap when the incident wave period is 1.60 s ($kh = 1.684$) and 1.17 s ($kh = 2.954$). These two diagrams illustrate that the free surface elevation with low wave frequency still keep

a linear wave shape, while the waves with high wave frequency tend to be non-linear. The discrepancies of HRAO in higher frequency region indicates that non-linear wave issues cannot be well resolved by linear potential flow theory-based method. Even though, the modified HAMS[®] with viscosity corrections can predict the general tendency of the curve of HRAO, and the values are generally close to the OpenFOAM[®] and experimental results. Thus, the parametric study used the modified HAMS[®] to predict forces and *CWR* under various conditions.

4 RESULTS AND DISCUSSIONS

The diagram of *CWR* in Figure 5 shows that the efficiency of wave energy extraction of the cylinder WEC can be improved significantly by the existence of the breakwater. In addition, different gap widths between the WEC and the breakwater affect the *CWR* as well. The WEC-B system with narrower gap widths has a higher *CWR* in general and the *CWR* keeps a high value in the wider range of *kh*. With the increase of the gap width, the maximum *CWR* decreases gradually, and the main peak also shifts to the lower wave frequency region (with smaller *kh*). When gap width reaches 0.4 m or bigger the second peak occurs and gets bigger with the increase of gap width. The curve of *CWR* when gap width is 0.6 m has an obvious second main peak, which is induced by the large wave excitation forces on the WEC structure in the high frequency region (shown in the left figure of Figure 5). The large wave excitation may be influenced by the Bragg reflection which refers to the extreme wave loads on structure occurred in the specific wave frequency due to the reflected waves by rear structures. This phenomenon was also observed in the previous parametric study by the authors (Ding et al., 2019).

Further parametric study on different geometries of WEC buoys and coaxial cylinder WEC buoys setup will be presented during the workshop.

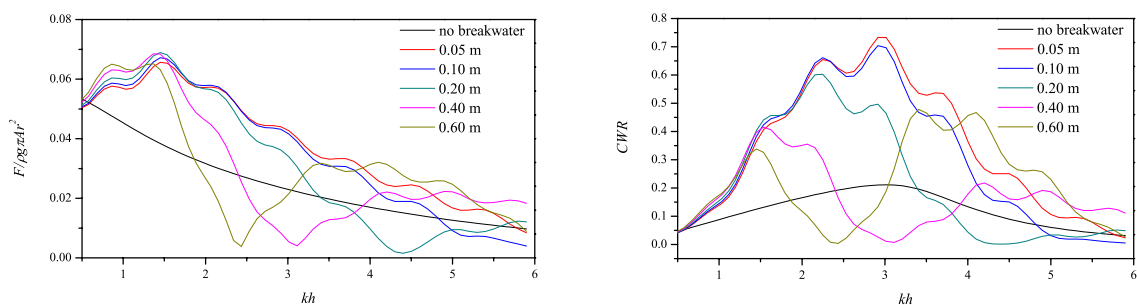


Figure 5. the dimensionless wave excitation force on the WEC (left) and capture width ratio (right) as a function of *kh*.

ACKNOWLEDGMENTS

The authors are very grateful for the support from the University of Bath HPC support team. The authors are also very grateful to Dr. Yingyi Liu for his support in using HAMS[®]. This research is financially supported by the Royal Academy of Engineering (RAE Grant No. UK-CIAPP/73).

REFERENCES

- Ding, H., Zang, J., Ning, D., Zhao, X., Chen, Q., Blenkinsopp, C. and Gao, J., 2019. Evaluation of the performance of an integrated WEC type of breakwater system. *the 38th International Conference on Ocean, Offshore & Arctic Engineering*, 9-14 June 2019, Glasgow, Scotland, UK.
- Jacobsen, N.G., Fuhrman, D.R., Fredsøe, J., 2012. A wave generation toolbox for the opensource CFD library: OpenFoam[®]. *International Journal of Numerical Method Fluids*, 70, pp.1073-1088.
- Liu, Y., 2019. HAMS: A frequency-domain preprocessor for wave-structure interactions – theory, development, and application. *Journal of Marine Science and Engineering*, 7(3), pp. 81-100.
- Liu, Y., Hu, C., Sueyoshi, M., Iwashita, H. and Kashiwagi, M., 2016. Motion response prediction by hybrid panel-stick models for a semi-submersible with bracings. *Journal of Marine Science and Technology*, 21, pp. 742-757.
- Zhao, X., Ning, D. and Liang, D., 2019. Experimental investigation on hydrodynamic performance of a breakwater-integrated WEC system. *Ocean Engineering*, 171, pp. 25-32.